Structural, Magnetic, and Gas Adsorption Study of a Two-Dimensional Tetrazole-Pyrimidine Based Metal–Organic Framework

ARTICLE *in* CRYSTAL GROWTH & DESIGN · MAY 2010

Impact Factor: 4.89 · DOI: 10.1021/cg1003726

4 AUTHORS:

Pradip S Pachfule
CSIR - National Chemical Laboratory, Pune
44 PUBLICATIONS **1,025** CITATIONS
SEE PROFILE

Raja Das
CSIR - National Chemical Laboratory, Pune
35 PUBLICATIONS **663** CITATIONS
SEE PROFILE

Pankaj Poddar
CSIR - National Chemical Laboratory, Pune
129 PUBLICATIONS **2,415** CITATIONS
SEE PROFILE

Rahul Banerjee
CSIR - National Chemical Laboratory, Pune
126 PUBLICATIONS **5,868** CITATIONS
SEE PROFILE

DOI: 10.1021/cg1003726

CRYSTAL GROWTH & DESIGN
Communication
2010, Vol. 10
2475–2478

Structural, Magnetic, and Gas Adsorption Study of a Two-Dimensional Tetrazole-Pyrimidine Based Metal−Organic Framework

Pradip Pachfule, Raja Das, Pankaj Poddar, and Rahul Banerjee*

Physical/Materials Chemistry Division, National Chemical Laboratory, Dr. Homi Bhaba Road, Pune 411008, India

Received March 20, 2010; Revised Manuscript Received April 26, 2010

ABSTRACT: A new two-dimensional (2D) metal−organic framework, Cu-TP-1, has been synthesized under solvothermal conditions (DMF) from the transition metal cation Cu(II) and 2-tetrazole pyrimidine ($C_5H_5N_6$, H-TP). The structure has been determined by single crystal X-ray crystallography which shows a (6,3) honeycomb 2D net with perpendicular one-dimensional channels. Permanent porosity of Cu-TP-1 has been determined by the nitrogen adsorption isotherm. Cu-TP-1 show interesting H_2 and CO_2 uptake. CO_2 uptake of Cu-TP-1 (at 298 K, 1 atm pressure) is seen to be comparable to the recently reported ZIF-95 which outperforms ZIF-100 and BPL carbon. The magnetic properties show an antiferromagnetically coupled Cu···Cu interaction down to 8 K with a Weiss temperature around 108 K.

Metal−organic frameworks (MOFs) have become an important class of materials as they cover a much wider range of pore sizes than zeolites and other microporous and mesoporous materials.[1] Moreover, a combination of organic and inorganic building blocks offers infinite number of variations, enormous flexibility in pore size and shape, and diverse opportunities for functionalization in MOFs. MOFs can be used in the area of gas storage and sequestration,[2] nonlinear optics (NLO),[3] sensors,[4] catalysis,[5] and magnetism.[6] A common design strategy for MOF materials exploits rigid and extended organic ligands such as carboxylates and polypyridines as an organic backbone. However, other ligands especially nitrogen-containing heterocyclic compounds (e.g., pyrazole, imidazoles, triazoles, and tetrazoles) have been exploited in the construction of complex metal organic architectures.[7] As these links are small in size, by adjusting the shape, flexibility, length, and symmetry, a remarkable range of MOFs containing various architectures and functions can be prepared.

Recently, researchers explored the structural chemistry of a series of metal imidazolates, triazolates, and tetrazolates.[8] These ligands lead to a diverse variety of MOFs as these ligands (a) have many potential coordination modes, allowing for the construction of a topologically diverse family of materials; (b) they are rigid, which helps enable the preparation of permanently porous materials; and (c) they have a compact structure that gives rise to the zeolitic pores suitable for gas storage and sequestration. To study the structural aspects using these types ligands, we chose 2-tetrazole pyrimidine or 5-(pyrimidyl) tetrazole ($C_5H_5N_6$, H-TP) as an organic building block containing both tetrazole and pyrimidine functionality. Although there are a few reports describing MOFs using this heterocyclic link, all of them illustrate the formation of either hydrogen bonded networks or 2D/3D structures without any significant porosity.[9] In this contribution, we report the structural analysis, magnetic properties, and gas adsorption studies of a porous MOF synthesized from 2-tetrazole pyrimidine or 5-(pyrimidyl) tetrazole and transition metal ion Cu(II) as a metal center in DMF media (Scheme 1). The MOF synthesized can be formulated as $[Cu(TP)_{1.5}(OH)_{0.5}]$ (**Cu-TP-1**) (TP = 5-(pyrimidyl) tetrazolate, DMF = dimethyl formamide) display an interesting two-dimensional (2D) architecture containing trapped H_2O molecules inside. The structure of Cu-TP-1 has been determined by single crystal X-ray crystallography and further identified by IR spectroscopy, powder X-ray diffraction (PXRD) and thermogravimetric analysis (TGA). Permanent porosity of Cu-TP-1 has been determined by the nitrogen adsorption isotherm. Cu-TP-1 also show interesting H_2 and CO_2 uptake.

Scheme 1. Schematic Diagram Showing Synthesis of 2-Tetrazole Pyrimidine and Cu-TP-1

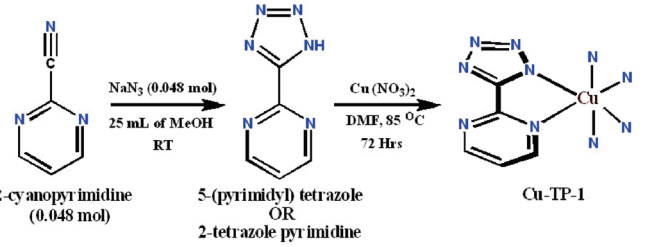

2-Tetrazole pyrimidine was synthesized according to a modified literature procedure. As 2-tetrazole pyrimidine is sparingly soluble in water at moderate temperature, we used the solvent DMF in which it is readily soluble. Also the reaction of it with $Cu(NO_3)_2$ at room temperature results in the formation of microcrystalline precipitate of Cu-TP-1. So we used the hydrothermal condition (at 85 °C) for synthesis which results in the formation of single crystals suitable for X-ray diffraction.[10] To a stock solution of 1.5 mL of 2-tetrazole pyrimidine (0.20 M) 0.5 mL of $Cu(NO_3)_2 \cdot 3H_2O$ (0.20 M) was added. To this solution was added 0.5 mL of absolute ethanol. The vial was capped and heated to 85 °C for 96 h (Scheme 1). The mother liquor was decanted and the products were washed with DMF (15 mL) three times. The as-synthesized Cu-TP-1 is stable and insoluble in common organic solvents. Further, thermal stability and phase purity of the bulk compound synthesized was checked by TGA and PXRD. Magnetic behavior was studied with the help of a vibrating sample magnetometer at a temperature range 5−350 K.

The asymmetric unit of Cu-TP-1 (space group $R\bar{3}c$) consists of two crystallographically independent Cu^{2+} ions, two 2-tetrazole pyrimidine (2-TP), and two lattice water molecules. Each Cu^{2+} ion is surrounded by six nitrogen atoms from three chelating 2-tetrazole pyrimidine where Cu−N distances range from 2.455(3) to 2.562(3) Å (Figure 1a). In the structure the Cu−$N_{tetrazole}$ distance [2.455(2) Å] is shorter than the Cu−$N_{pyrimidine}$ distance [2.562 (3) Å] as it originates from the deprotonated tetrazole ring, whereas the pyrimidine ring fulfills the co-ordination of the metal ion. Six TP ligands link to six Cu^{2+} ions in a 6-membered ring which further extends into a (6,3) honeycomb

*To whom correspondence should be addressed. E-mail: r.banerjee@ncl.res.in. Fax: + 91-20-25902636. Tel: + 91-20-25902535.

Published on Web 05/04/2010

2D net on the *ab* plane as shown in Figure 1b. The pyrimidine and tetrazole rings of TP ligands hang on both sides of the sheet (Figure 1c). Within the layers, Cu···Cu distances across the TP ligands and through the diagonal of the hexagonal ring are ~5.88, ~10.49, and ~11.93 Å, respectively.[11] It should be noted that the (6,3) sheets are stacked in a face-to face fashion along the *c*-axis with 1D channels in which H_2O molecules are embedded, and the shortest Cu···Cu interlayer separation along the *c*-axis is ca. 7.0 Å. This is the first example of a porous 2D honeycomb network with this ligand as all the other MOFs with this link possess nonporous architectures. The structure contains interesting hexagonal 1D channels; in each channel three pyrimidine and three tetrazole rings protrude inside. The dimension of these hexagonal channels along the crystallographic *a*-axis is about 12.1 Å. The calculations using PLATON[12] suggest a 25.2% void space of the total crystal volume after removal of guest and coordinated water molecules, respectively.

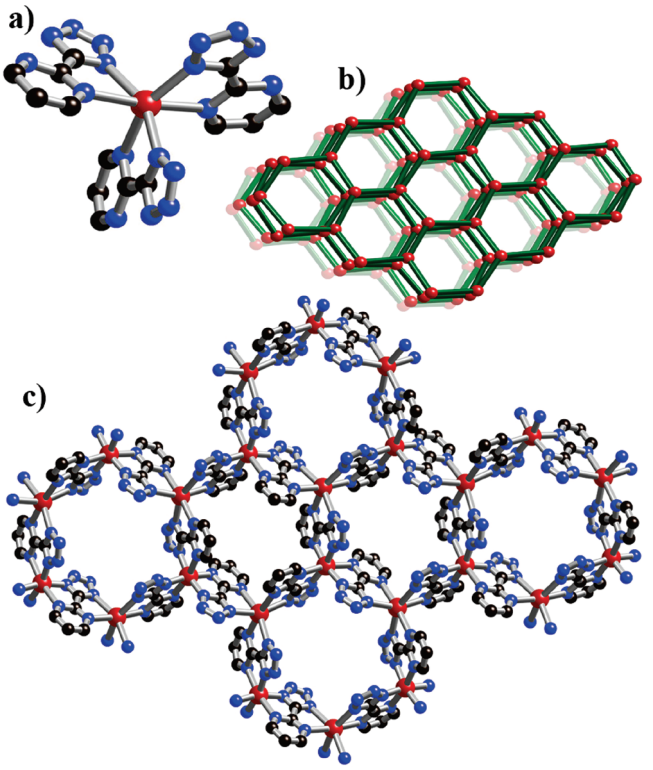

Figure 1. (a) Structure of Cu-TP-1. (a) Ball-and-stick representation of the SBU of Cu-TP-1 showing the coordination environment around Cu. (b) (6,3) honeycomb 2D net on the *ab* plane of Cu-TP-1. (c) Packing diagram of Cu-TP-1 representing the (6,3) honeycomb 2D net on the *ab* plane. Color code: Cu (dark red), N (blue), C (black).

To examine the architectural and thermal stability of Cu-TP-1, we prepared this at gram scale to allow detailed investigation of the aforementioned properties. TGA performed on the as-synthesized Cu-TP-1 revealed that this compound has high thermal stability (see Section S3 in Supporting Information, for all data and interpretations regarding guest mobility and thermal stability of Cu-TP-1) as no strictly clean weight loss step occurred below 300 °C. The TGA trace Cu-TP-1 showed a gradual weight loss step of 13.9% (15−300 °C), corresponding to the escape of all H_2O molecules trapped in the pores of MOF (2 H_2O; calcd. 11.1%). A sharp weight loss at 300 °C indicates decomposition of the host framework. In order to confirm the phase purity of the bulk materials, PXRD experiments were carried out for this MOF. The PXRD experimental and computer-simulated patterns of all of them are shown in Supporting Information (Figure S1). As shown in figure, all major peaks of experimental powder X-ray patterns (PXRDs) of matches quite well that of simulated PXRDs, indicating their reasonable crystalline phase purity.

The permanent porosity of guest-free (activated) Cu-TP-1 was confirmed by gas adsorption measurements. As-synthesized Cu-TP-1 consists of approximately 13 wt % H_2O molecules, as quantified from TGA (see Supporting Information, Figure S3). An as-synthesized sample of Cu-TP-1 was immersed in dry chloroform at ambient temperature for 72 h, evacuated at ambient temperature for 24 h, then at an elevated temperature (85 °C) for 48 h. The sample thus obtained was optimally evacuated, as evidenced by their well-maintained PXRD patterns and the long plateau (ambient temperature to 300 °C) in their TGA traces. The type-I isotherm (International Union of Pure and Applied Chemistry classification) observed for N_2 adsorption at 77 K (Figure 2a) indicates the microporosity of activated Cu-TP-1. The small H_4 hysteresis at relative pressure $P/P_0 > 0.5$ (where P_0 is the saturated vapor pressure of the adsorptive at the temperature of measurement and P is the equilibrium pressure) can be attributed to intercrystalline voids in the sample.[13] The maximum pore aperture (3.7 Å) of Cu-TP-1, as measured from its crystal structure, is comparable to the kinetic diameter of N_2 (3.6 Å). However, the space inside the structure becomes accessible through a dynamic aperture-widening process wherein the aromatic ring swings out of the way to allow gas molecules to pass. The apparent surface area and pore volume were calculated to be 258 and 286 $m^2\ g^{-1}$ by applying the BET and Langmuir equation, respectively.[14] It is now commonly believed that carbon dioxide emissions from burning of fossil fuels in power plants and automobiles are altering the temperature of the atmosphere and the acidity of the oceans with undesirable consequences for the Earth's environment.[15] It has been shown that MOFs and ZIFs can hold large amounts of gases, including carbon dioxide, and that gas uptake can be selective.[8,16] We studied the CO_2 uptake of

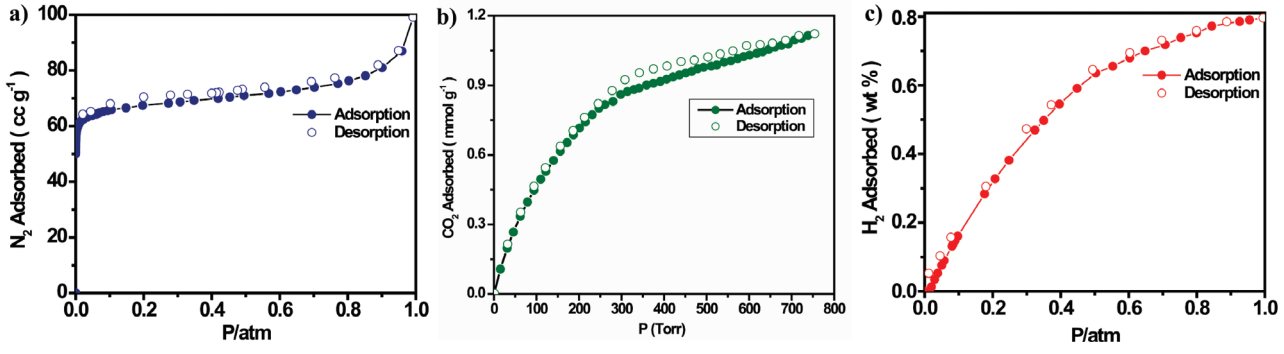

Figure 2. Gas adsorption isotherms of Cu-TP-1. N_2 at 77 K (blue circles, a); CO_2 (green, circles, b) at 298 K, and H_2 (red circles, c) at 77 K for Cu-TP-1; the filled and open shapes represent adsorption and desorption, respectively. P/P_0, relative pressure at the saturation vapor pressure of the adsorbate gas.

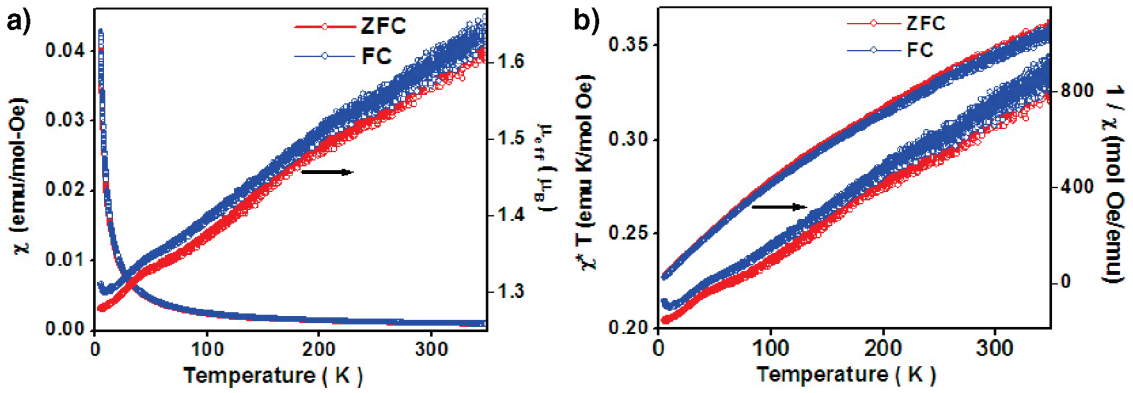

Figure 3. The temperature dependence of the (a) magnetic susceptibility χ (left axis) and the effective magnetic moment μ_{eff} (right axis); (b) χT (left axis) and $1/\chi$ (right axis) for as-synthesized Cu-TP-1 reported in the paper.

Cu-TP-1 as it contains free nitrogen which according to a recent theoretical study should enhance the adsorption energy of CO_2.[17] CO_2 uptake of Cu-TP-1 is seen to be comparable to recently reported ZIF-95 which outperforms ZIF-100 and BPL carbon (Figure 2b).[18,8e] Although some zeolite materials outperform BPL carbon in terms of selective CO_2 adsorption, regeneration difficulties mean that their suitability for practical use is uncertain and they were therefore not included in the comparative adsorption measurements.[19] Figure 2b also illustrates that both Cu-TP-1 show complete reversibility of adsorption and desorption of CO_2. More detailed analysis of the data in Figure 2b indicates that one gram of Cu-TP-1 can hold up to 25.2 cc per gram (or 1.2 mmol per g) of CO_2 at 298 K and ambient pressure.[20] Adsorption isotherms for H_2 were collected at 77 K as shown in Figure 2c. It should be noted that the repeatability of the H_2 adsorption behavior was confirmed by reproducing the same isotherm three times at 77 K. The uptake at ~800 Torr at 77 K is 0.8 wt % which is comparable with some porous MOFs with small pores.[21]

DC magnetization vs temperature measurements were performed for Cu-TP-1 at 500 Oe in both field cooled (FC) and zero field cooled (ZFC) modes. For the FC and ZFC measurements, the sample was cooled to 5 K in a 500 Oe field and without field, respectively, and data were collected while heating in both cases at 2 K per minute at every second after averaging over 40 Hz. Temperature dependence of ZFC and FC molar magnetic susceptibility (χ) shows the overlapping of ZFC and FC on each other in the measured temperature range (Figure 3a). The effective magnetic moment, μ_{eff} vs T curves show a sharply decreasing trend in μ_{eff} with decreasing temperature probably due to an antiferromagnetic superexchange interaction between Cu^{2+} ions followed by an increase in the μ_{eff} value as the temperature goes below 8 K. At 300 K, value of μ_{eff} is 1.6 μ_B/Cu atom which is almost equal to the theoretical calculated value for one Cu^{2+} ion (1.73 μ_B). The slight decrease in the value indicates the onset of antiferromagnetic ordering. The value of χT at 350 K is 0.33 emu mol^{-1} K and decreases with decreasing temperature with a minimum around 8 K, followed by an increase until the lowest measured temperature. The increase in the values of μ_{eff} as well χT indicates the probable domination of $Cu^{2+}\cdots Cu^{2+}$ ferromagnetic coupling over antiferromagnetic coupling due to the reduced thermal activation energy at a temperature below 8 K. The temperature dependence of $1/\chi$ shows Curie−Weiss behavior until 180 K with a Curie constant $C = 0.44$ emu K/mol Oe and Weiss temperature $\theta = 109$ K, and below 180 K, it deviates from Curie−Weiss behavior probably due to temperature-dependent modifications into antiferromagnetic interaction pathways.

In conclusion, we have successfully synthesized and characterized one 2D porous metal−organic framework with an interesting (6,3) topology where the Cu^{2+} show dominantly antiferromagnetic coupling mediated by the organic framework down to ~8 K followed by a small ferromagnetic like upturn in magnetization. To our knowledge, this is the first report of a porous 2D MOF with this organic backbone. This result once again proves that there lies an immense potential of synthesizing MOFs with noncarboxylate building blocks. We believe that these findings will not only be useful at the basic level in the crystal engineering of coordination networks but also enrich the database of MOFs having noncarboxylate organic building units. We are continuing to utilize other substituted, neutral nitrogen-donor ligands to rationally design and synthesize new MOFs with specific structure and properties.

Acknowledgment. P.P. acknowledges CSIR for a project assistantship (PA-II) from CSIR's XIth Five Year Plan Project (NWP0022-H). R.B. acknowledges Dr. S. Sivaram, Director NCL for start-up grants and CSIR's XIth Five Year Plan Project (Grant No. NWP0022-H) for funding and also Dr. S. Pal and Dr. K. Vijaymohanan and Dr. V. G. Puranik for their encouragement. Financial assistance from the DST (SR/S1/IC-22/2009) and (SR/S5/NM-104/2006) is acknowledged.

Supporting Information Available: Description of experimental details, including synthetic methods, crystallography, supplementary figures, including TGA, powder XRD profiles, tables of crystallographic data, and CIF files and thermal ellipsoids for MOF reported in this paper. This material is available free of charge via the Internet at http://pubs.acs.org.

References

(1) (a) Sudik, A.-C.; Côté, A.-P.; Wong-Foy, A. G.; O'Keeffe, M.; Yaghi, O. M. *Angew. Chem., Int. Ed.* **2006**, *45*, 2528. (b) Kondo, A.; Noguchi, H.; Kajiro, H.; Carlucci, L.; Mercandelli, P.; Proserpio, D. -M.; Respiration, M. *J. Phys. Chem. B.* **2006**, *110*, 25565. (c) Hong, M. *Cryst. Growth Des.* **2007**, *7*, 10. (d) Janiak, C. *Dalton Trans.* **2003**, *14*, 2781. (e) Rao, C. N. R.; Cheetham, A. K.; Thirumurugan, A. *J. Phys.: Condens. Matter* **2008**, *20*, 083202. (f) Robson, R. *Dalton Trans.* **2008**, 5113. (g) Eddaoudi, M.; Kim, J.; Rosi, N.; Vodak, D.; Wachter, J.; O'Keeffe, M.; Yaghi, O. M. *Science* **2002**, *295*, 469.

(2) (a) Bastin, L.; Bárcia, P.-S.; Hurtado, E.-J.; Silva, J.-A.; Rodrigues, A.-E.; Chen, B.-L. *J. Phys. Chem. C.* **2008**, *112*, 1575. (b) Kumar, D.-K.; Das, A.; Dastidar, P. *Cryst. Growth Des.* **2007**, *7*, 205. (c) Hu, S.; Zhang, J.-P.; Li, H.-X.; Tong, M.-L.; Chen, X.-M.; Kitagawa, S. *Cryst. Growth Des.* **2007**, *7*, 2286. (d) Chen, B.-L.; Ma, S.-Q.; Zapata, F.; Fronczek, F.-R.; Lobkocsky, E.-B.; Zhou, H.-C. *Inorg. Chem.* **2007**, *46*, 1233. (e) Kitagawa, S.; Kitaura, R.; Noro, S. *Angew. Chem., Int. Ed.* **2004**, *43*, 2334. (f) Thallapally, P. K.; Tian, J.; Motkuri, R. K.; Fernandez, C. A.; Dalgarno, S. J.; McGrail, P. B.; Warren, J. E.; Atwood, J. L. *J. Am. Chem. Soc.* **2008**, *130*, 16842. (g) Mckinlay, R. M.; Thallapally, P. K.; Atwood, J. L. *Chem. Commun.* **2006**, 2956. (h) Motkuri, R. K.; Tian, J.; Thallapally, P. K.; Fernandez, C. A.; Dalgarno, S. J.; Warren, J. E.; McGrail, P. B.; Atwood, J. L. *Chem. Commun.* **2010**, *46*, 538. (i) Thallapally, P. K.; Fernandez, C. A.;

Motkuri, R. K.; Nune, S. K.; Liu, J.; Peden, C. H. F. *Dalton Trans.* **2010**, *39*, 1692.
(3) Myers, L.-K.; Langhoff, C.; Thompson, M.-E. *J. Am. Chem. Soc.* **1992**, *114*, 7560.
(4) (a) He, J.-H.; Yu, J.-H.; Zhang, Y.-T.; Pan, Q.-H.; Xu, R.-R. *Inorg. Chem.* **2005**, *44*, 9279. (b) Yang, E.-C.; Zhao, H.-K.; Ding, B.; Wang, X.-G.; Zhao, X.-J. *Cryst. Growth Des.* **2007**, *7*, 2009. (c) Bauer, C.-A.; Timofeeva, T.-V.; Settersten, T.-B.; Patterson, B. D.; Liu, V.-H.; Simmons, B.-A.; Allendorf, M.-D. *J. Am. Chem. Soc.* **2007**, *129*, 7136. (d) Sun, D.-F.; Ke, Y.-X.; Collins, D.-J.; Lorigan, G.-A.; Zhou, H.-C. *Inorg. Chem.* **2007**, *46*, 2725.
(5) (a) Wu, C. D.; Hu, A.; Zhang, L.; Lin, W. B. *J. Am. Chem. Soc.* **2005**, *127*, 8940. (b) Lin, W. B. *J. Solid State Chem.* **2005**, *178*, 2486. (c) Fujita, M.; Kwon, Y. J.; Washizu, S.; Ogura, K. *J. Am. Chem. Soc.* **1994**, *116*, 1151. (d) Seo, J. S.; Whang, D.; Lee, H.; Jun, S. I.; Oh, J.; Jeon, Y. J.; Kim, K. *Nature* **2000**, *404*, 982. (e) Ohmori, O.; Fujita, M. *Chem. Commun.* **2004**, *10*, 1586. (f) Lin, W. *MRS Bull.* **2007**, *32*, 544.
(6) (a) Poulsen, R.-D.; Bentien, A.; Chevalier, M.; Iversen, B.-B. *J. Am. Chem. Soc.* **2005**, *127*, 9156. (b) Ghosh, S.-K.; Ribas, J.; Fallah, M.-S.; Bharadwaj, P.-K. *Inorg. Chem.* **2005**, *44*, 3856. (c) Xiang, S.-C.; Wu, X.-T.; Zhang, J.-J.; Fu, R.-B.; Hu, S.-M.; Zhang, X.-D. *J. Am. Chem. Soc.* **2005**, *127*, 16352. (d) Luo, F.; Hu, D.-X.; Xue, L.; Che, Y.-X.; Zheng, J.-M. *Cryst. Growth Des.* **2007**, *7*, 851.
(7) (a) Zhang, J. P.; Lin, Y.-Y.; Zhang, W.-X.; Chen, X.-M. *J. Am. Chem. Soc.* **2005**, *127*, 14162. (b) Patel, R.; Weller, M. T.; Price, D. J. *Dalton Trans.* **2007**, 4034. (c) Wang, Y.; Ding, B.; Cheng, P.; Liao, D.-Z.; Yan, S.-P. *Inorg. Chem.* **2007**, *46*, 2002. (d) Dinca, M.; Dailly, A.; Tsay, C.; Long, J. R. *Inorg. Chem.* **2008**, *47*, 11. (e) Zhang, J.-P.; Chen, X. M. *Chem. Commun.* **2006**, 1689. (f) Zhao, H.; Qu, Z.-R.; Ye, H.-Y.; Xiong, R.-G. *Chem. Soc. Rev.* **2008**, *37*, 84.
(8) (a) Park, K. S.; Zheng, N.; Cöté, A.-P.; Choi, J. Y.; Huang, R.; Uribe-Romo, F. J.; Chae, H. K.; O'Keeffe, M.; Yaghi, O. M. *Proc. Natl. Acad. Sci. U.S.A.* **2006**, *103*, 10186. (b) Huang, X.-C.; Lin, Y.-Y.; Zhang, J.-P.; Chen, X.-M. *Angew. Chem., Int. Ed.* **2006**, *45*, 1557. (c) Banerjee, R.; Phan, A.; Wang, B.; Knobler, C.; Furukawa, H.; O'Keeffe, M.; Yaghi, O. M. *Science* **2008**, *319*, 939. (d) Hayashi, H.; Cöté, A.-P.; Furukawa, H.; O'Keeffe, M.; Yaghi, O. M. *Nat. Mater.* **2007**, *6*, 501. (e) Wang, B.; Cöté, A. P.; Furukawa, H.; O'Keeffe, M.; Yaghi, O. M. *Nature* **2008**, *453*, 207.
(9) (a) Zhang, J.-Y.; Yue, Q.; Jia, Q.-X.; Cheng, A.-L.; Gao, E.-Q. *CrystEngComm* **2008**, *10*, 1443–1449. (b) Li, J.-R.; Yu, Q.; Sanido, E. C.; Tao, Y.; Song, W.-C.; Bu, X.-H. *Chem. Mater.* **2008**, *20*, 1218–1220. (c) Zhang, J.-Y.; Cheng, A.-L.; Yue, Q.; Sun, W.-W.; Gao, E.-Q. *Chem. Commun.* **2008**, 847–849.
(10) The single crystal data was collected on Bruker APEX CCD X-ray diffractometer that uses graphite monochromated Mo Kα radiation (λ = 0.71073 Å). Crystal data for Cu-TP-1: Hexagonal, $R\bar{3}c$, a = 17.967(3) Å, b = 17.967(3) Å, c = 42.438(9) Å, V = 11864(4) Å^3, D_c = 1.418 g cm^{-3}, 2232 reflections out of 6742 unique reflections with $I > 2\sigma(I)$, $1.62 < \theta < 25.00$, final R-factors R_1 = 0.0844, wR_2 = 0.2174. Crystal data and details of data collection, structure solution, and refinement are summarized in Supporting Information. Crystallographic data (excluding structure factors) for the structure reported in this paper has been deposited with the CCDC as deposition No. CCDC 770370. Copy of the data can be obtained, free of charge, on application to the CCDC, 12 Union Road, Cambridge CB2 lEZ UK (fax: + 44 (1223) 336 033; e-mail: deposit@ccdc.cam.ac.uk).
(11) All calculation were done using Cerius^2 software (Ver. 4.2, Accelrys); van der Waals radii were taken into consideration in all cases (C, 1.70; H, 1.20; O, 1.52; N, 1.55; Å).
(12) Spek, A. L. *PLATON, A Multipurpose Crystallographic Tool*; Utrecht University: Utrecht, The Netherlands, 2005.
(13) Vishnyakov, A.; Ravikovitch, P. I.; Neimark, A. V.; Bülow, M.; Wang, Q. M. *Nano Lett.* **2003**, *3*, 713–718.
(14) Rouquerol, F.; Rouquerol, J.; Sing, K. *Adsorption by Powders & Porous Solids*; Academic Press: London, 1999.
(15) Houghton, J. T.; Meira Filho, L. G.; Griggs, D. J.; Noguer, M. *Implications of Proposed CO_2 Emissions Limitations*, Technical Paper IV, IPCC, Geneva, Switzerland, 1997.
(16) (a) Li, H.; Eddaoudi, M.; Groy, T. L.; Yaghi, O. M. *J. Am. Chem. Soc.* **1998**, *120*, 8571–8572. (b) Millward, A. R.; Yaghi, O. M. *J. Am. Chem. Soc.* **2005**, *127*, 17998–17999. (c) An, J.; Geib, S. J.; Rosi, N. L. *J. Am. Chem. Soc.* **2010**, *132* (1), 38–39.
(17) Vogiatzis, K. D.; Mavrandonakis, A.; Klopper, W.; Froudakis, G. E. *ChemPhysChem* **2009**, *10*, 374.
(18) Sircar, S.; Golden, T. C.; Rao, M. B. *Carbon* **1996**, *34*, 1.
(19) Sircar, S. *Ind. Eng. Chem. Res.* **2006**, *45*, 5435.
(20) It is noteworthy that some MOFs and ZIFs (namely, ZIF-69 and ZIF-76) have a higher overall capacity and selectivity for carbon dioxide.
(21) (a) Rowsell, J. L. C.; Yaghi, O. M. *J. Am. Chem. Soc.* **2006**, *128*, 1304–1315. (b) Dincă, M.; Yu, A. F.; Long, J. R. *J. Am. Chem. Soc.* **2006**, *128*, 8904–8913.